Mechanistic Studies of Ni-Catalyzed Electrochemical Homo-Coupling Reactions of Aryl Halides

Jian Luo, Michael T. Davenport, Arianna Carter, Daniel H. Ess, and T. Leo Liu a

- a. Department of Chemistry and Biochemistry, Utah State University, Logan, Utah 84322
- b. Department of Chemistry and Biochemistry, Brigham Young University, Provo, Utah 84604

 Corresponding: dhe@chem.byu.edu, leo.liu@usu.edu

Abstract: Ni-catalyzed electrochemical arylation is an attractive, emerging approach for molecular construction as it uses air-stable Ni catalysts and efficiently proceeds at room temperature. However, the homo-coupling of aryl halide substrates is one of the major side reactions. Herein, extensive experimental and computational studies were conducted to examine the mechanism of Ni-catalyzed electrochemical homo-coupling of aryl halides. The results indicate that an unstable Ni^{II}(Ar) intermediate formed through oxidative addition of the cathodically generated Ni^I species with aryl bromide and a consecutive chemical reduction step. For electron-rich aryl halides, homo-coupling reaction efficiency is limited by the oxidative addition step, which can be improved by negatively shifting the redox potential of the Ni-catalyst. DFT computational studies suggest a Ni^{III}(Ar)/Ni^{II}(Ar) ligand exchange pathway for the formation of high-valence Ni^{III}(Ar)₂ intermediate for reductive elimination and production of the biaryl product. This work reveals the reaction mechanism of Ni-catalyzed electrochemical homo-coupling of aryl halides, which may provide valuable information for developing cross-coupling reactions with high selectivity.

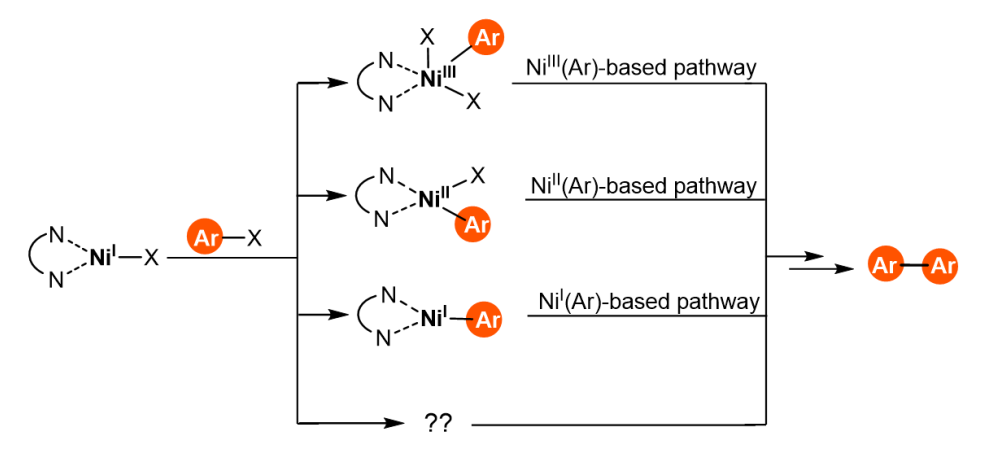
Aryl groups widely exist in various chemicals and represent the basic backbone or essential functional groups for molecules or materials. Therefore, arylation reaction is one of the core strategies for molecular construction in contemporary synthetic chemistry. ¹⁻⁴ Ni-catalyzed electrochemical arylation between aryl halides and nucleophiles has attracted great attention due to its merits of using non-precious transition-metal catalysts, mild reaction conditions, controllable reaction process, and using electrical energy to drive chemical transformations, thereby avoiding

the use of stoichiometric chemical oxidants or reductants.⁵⁻⁸ Literature has witnessed the rapid development of Ni-catalyzed electrochemical arylation reactions, including arylation of alkyl halides,⁹⁻¹³ carboxylates,¹⁴⁻¹⁶ amines,^{8,17,18} alcohols,¹⁹ thiol,^{20,21} olefins,²²⁻²⁴ carbon dioxide,^{25,26} etc.

Scheme 1. Ni-Catalyzed Electrochemical Cross-Coupling Reactions and the Undesired Homo-Coupling Side Reactions

(A) Ni-catalyzed cross-coupling reactions

(B) Possible pathways for the production of aryl-aryl homo-coupling product



However, low yields and side reactions were observed in the Ni-catalyzed electrochemical arylation reactions via cross-coupling. 5,12,13,27 One of the major side reactions is the homo-coupling of aryl halides (Scheme 1A). 7,9,27 Under reducing conditions, biaryl products are produced via symmetrical coupling of aryl halides, which makes the cross-coupling reaction challenging for nucleophiles with low reactivity. 27 Although the Ni-catalyzed electrochemical homo-coupling of aryl halides has been applied in the synthesis of polypyridine ligands and axially chiral BINOL derivatives, 28-31 the flat symmetric biaryl structure of products limited the broad application of this reaction. To achieve high selectivity for cross-coupling products, suppression of aryl-aryl homo-coupling side reactions is expected, which requires in-depth mechanistic understanding of this competitive reaction. There are several possible pathways for the formation of biaryl products

under electrolytic conditions. As shown in Scheme 1B, the oxidative addition of cathodic reduction generated Ni^I species to aryl halide yields a Ni^{III}(Ar) species.^{7,17} The Ni^{III}(Ar) species can then decompose to produce the biaryl products via a bimolecular pathway. Alternatively, the Ni^{III}(Ar) species can be further reduced (chemically or electrochemically) to either a Ni^{II}(Ar) or a Ni^I(Ar) species and then be converted to the biaryl products.

Herein, we conducted experimental and computational studies to elucidate the mechanism of Ni-catalyzed electrochemical homo-coupling of aryl halides. Our results indicate that an unstable Ni^{II}(Ar) intermediate formed through the oxidative addition of aryl bromide to the cathodicaly generated Ni^I species and a consecutive chemical reduction step. For electron-rich aryl halides, homo-coupling reaction efficiency is limited by the oxidative addition step, which can be improved by using electron-rich ligands for a Ni-catalyst. DFT computational studies suggest a Ni^{III}(Ar)/Ni^{II}(Ar) ligand exchange pathway for the formation of a high-valence Ni^{III}(Ar)₂ intermediate for reductive elimination and production of the biaryl product.

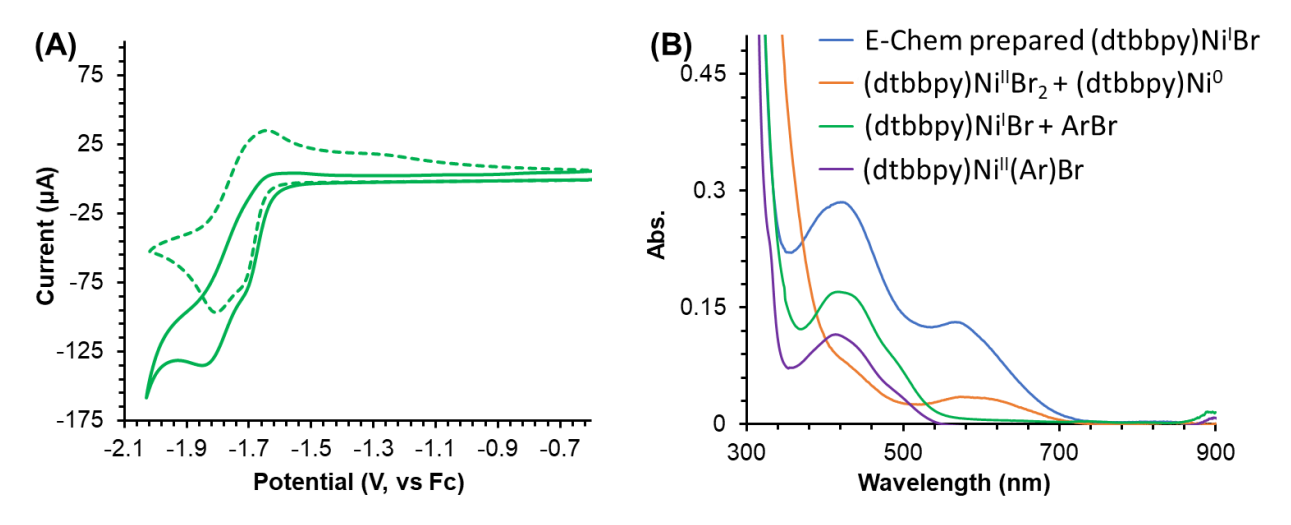


Figure 1. Electrochemical and UV-Vis studies of Ni-catalyzed aryl halide homo-coupling. (A) Cyclic voltammograms (CV) of the Ni-catalyst with (solid line) and without (dash line) methyl 4-bromobenzoate; (B) UV-Vis spectra of electrochemically prepared (blue) and chemically prepared (orange) (dtbbpy)Ni^IBr species, a mixture of (dtbbpy)Ni^IBr and 1 eq. ArBr (green), and chemically synthesized (dtbbpy)Ni^{II}(Ar)Br (purple).

As shown in Figure 1A, NiBr₂.DME/dtbbpy (1 : 1.5) catalyst showed a quasi-reversible redox signal with $E_{1/2} = -1.78$ V (vs. ferrocene/ferrocenium (Fc^{+/0})) (dashed curve) standing for the Ni^{II/I} redox couple. After adding 10 eq. aryl bromide, methyl 4-bromobenzoate, the reductive peak

current intensity was obviously increased, meanwhile, the return peak disappeared. It indicates an irreversible oxidative addition reaction between cathodically generated (dtbbpy)Ni^IBr species and the aryl halide. It is consistent with our previous results. To further confirm the oxidative addition of the aryl halide to the Ni^I species, we synthesized the (dtbbpy)Ni^IBr species through controlled potential electrolysis (CPE) of (dtbbpy)Ni^{II}Br₂ (see SI for detail). As shown in Figure 1B, UV-Vis absorption of the (dtbbpy)Ni^IBr species displayed three absorption peaks at 395 nm, 421 nm, and 568 nm (blue curve), respectively, which is consistent with the literature.³² We also tried to prepare the Ni^I species chemically by mixing (dtbbpy)Ni⁰ and (dtbbpy)Ni^{II}Br₂ (1 : 1). However, it is interesting that weak absorption peaks were observed at 433 nm, 577 nm, and 621 nm (orange curve) in the UV-Vis absorptions of (dtbbpy)Ni⁰/(dtbbpy)Ni^{II}Br₂ mixture. It indicates that almost no (dtbbpy)Ni¹Br species was generated in the comproportionation of (dtbbpy)Ni⁰ and (dtbbpy)Ni^{II}Br₂. The main product of this reaction is likely to be a Ni^I dimer, [(dtbbpy)Ni^IBr₂, which shows no UV-Vis absorption peak in the visible light range.³² The Ni^I dimer species was reported to be unreactive towards aryl halide oxidative addition.³² We further reacted aryl bromide with the electrochemically synthesized (dtbbpy)Ni^IBr species. A (dtbbpy)Ni^{II}(Ar)Br intermediate quickly formed through oxidative addition and subsequent chemical reduction, as UV-Vis of the mixture (green curve) is identical to that of independently synthesized (dtbbpy)Ni^{II}(Ar)Br (purple curve). The (dtbbpy)Ni^{II}(Ar)Br intermediate showed a main UV-Vis absorption peak at 416 nm and two shoulder peaks at 435 and 495 nm, respectively.

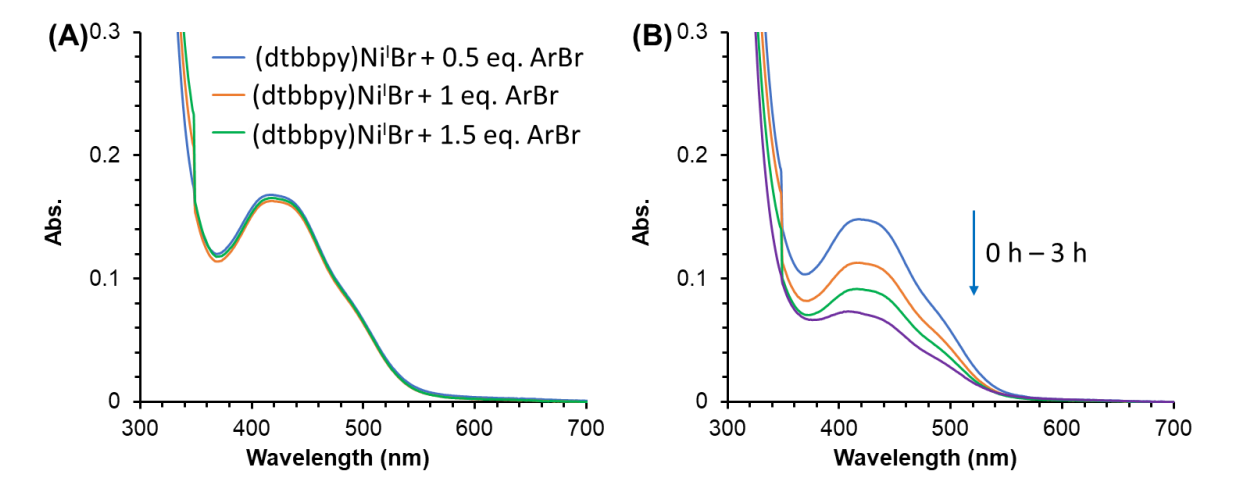


Figure 2. UV-Vis studies of the (dtbbpy)Ni^{II}(Ar)Br intermediate. (A) UV-Vis absorption of (dtbbpy)Ni^IBr reacted with 0.5 eq, 1 eq., and 1.5 eq. ArBr; (B) Stability tests of the (dtbbpy)Ni^{II}(Ar)Br intermediate ((dtbbpy)Ni^IBr/ArBr 1 : 1).

To monitor the reaction between Ni¹ species and aryl bromide, we titrated the (dtbbpy)Ni¹Br species with aryl bromide. As shown in Figure 2A, when the (dtbbpy)Ni¹Br species was mixed with 0.5 − 1.5 equivalent methyl 4-bromobenzoate, UV-Vis absorption of the mixtures was nearly identical. It indicates that, as shown in Scheme 2, when (dtbbpy)Ni¹II(Ar)Br₂ is formed via oxidative addition between (dtbbpy)Ni¹Br species and aryl bromide, it is rapidly converted to (dtbbpy)Ni¹I(Ar)Br through a comproportionation reaction with (dtbbpy)Ni¹Br species. The overall reaction is 2(dtbbpy)Ni¹Br + ArBr → (dtbbpy)Ni¹I(Ar)Br + (dtbbpy)Ni¹IBr₂. Therefore, despite the addition of more than 0.5 equivalent aryl bromide, the concentration of (dtbbpy)Ni¹I(Ar)Br intermediate in the mixture didn't increase. The (dtbbpy)Ni¹I(Ar)Br intermediate was found to be unstable in DMAc at room temperature. As shown in Figure 2B, a significant decrease in UV-Vis absorption of the (dtbbpy)Ni¹I(Ar)Br intermediate was observed, indicating its gradual decomposition over several hours. After 12 h, homo-coupling biaryl product, dimethyl [1,1'-biphenyl]-4,4'-dicarboxylate, was detected in the (dtbbpy)Ni¹Br/ArBr (1 : 1) mixture with 62% yield.

Scheme 2. Oxidative Addition and Subsequent Chemical Reduction between Ni^I Species and Aryl Bromide.

The above experimental results demonstrate a Ni^I-based oxidative addition pathway for Ar–Br bond activation, which is distinct from the previously proposed Ni⁰-based oxidative addition mechanism. ^{9,28} We further questioned how to accelerate the oxidative addition step of aryl halides to Ni^I species, especially for less reactive electron-rich aryl halides such as 4-bromo-N,N-dimethylaniline. In the oxidative addition reaction, Ni^I species and aryl halides act as a reductant and an oxidant, respectively. Thus, we hypothesized that negatively shifting the reduction potential of the Ni^I species could improve its reactivity towards electron-rich aryl halide. As shown in Figure 3, when 2,2'-bpy was used as ligand for the Ni-catalyst, a fully reversible redox signal of Ni(2,2'-bpy)₃^{2+/+} couple was observed at $E_{I/2} = -1.60$ V (vs. Fc) (orange dash). After adding 10 eq. 4-bromo-N,N-dimethylaniline, the reduction peak at $E_{I/2} = -1.71$ V was slightly increased, and the oxidation peak at -1.51 V was slightly decreased (orange solid), indicating a very slow oxidative addition reaction. When we replaced the 2,2'-bpy ligand with an electro-rich 4,4'-dimethoxy-2,2'-

bipyridyl (dmobpy) ligand, the redox potential of Ni(dmobpy)₃^{2+/+} redox couple negatively shifted to $E_{I/2} = -1.93$ V (vs. Fc) (green dash). Meanwhile, a stronger current response for the oxidative addition reaction was detected (green solid).

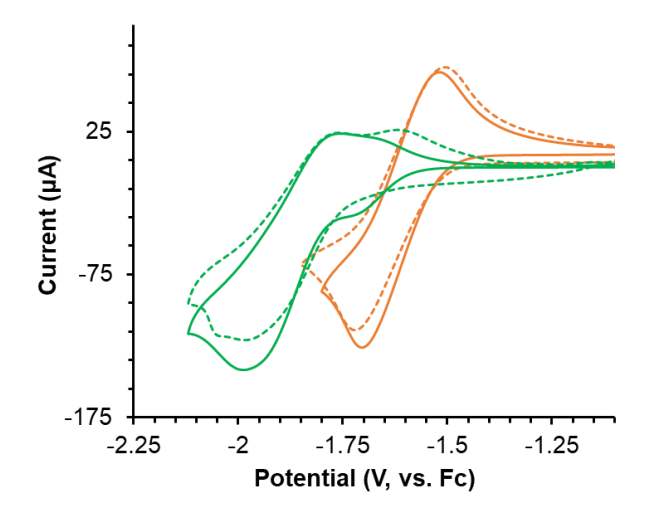


Figure 3. Cyclic voltammetry (CV) studies of a Ni-catalyzed electrochemical homo-coupling reaction of electron-rich 4-bromo-N,N-dimethylaniline. Ni(2,2'-bpy)₃Br₂ (orange dash), Ni(2,2'-bpy)₃Br₂ + ArBr (orange solid), Ni(dmobpy)₃Br₂ (green dash), Ni(dmobpy)₃Br₂ + ArBr (green solid).

Constant current electrolysis of 4-bromo-N,N-dimethylaniline with a Ni-catalyst was performed by using glassy carbon (RVC) as a cathode and Zn metal as a sacrificial anode. As shown in Scheme 3, in the presence of Ni(2,2'-bpy)₃Br₂ catalyst, the homo-coupling product, N⁴,N⁴,N⁴,N⁴-tetramethyl-[1,1'-biphenyl]-4,4'-diamine, was obtained in 54% yield after electrolysis at 4 mA current for 12 hours. 33% of 4-bromo-N,N-dimethylaniline remained in the reaction mixture. When Ni(dmobpy)₃Br₂ catalyst was used for the same reaction, 4-bromo-N,N-dimethylaniline was completely converted within 12 hours. The homo-coupling product was obtained with 81% yield. These results suggest that the reaction rate of the oxidative addition step and reaction efficiency of homo-coupling of electron-rich aryl halides can be enhanced by negatively shifting the redox potential of the Ni-catalyst or generating an electron-rich Ni¹ intermediate.

Scheme 3. Ni-Catalyzed Electrochemical Homo-Coupling Reactions of Electron-Rich Aryl Bromide

To reveal the details of reaction mechanism, we used M06/6-31G**(LANL2DZ for Ni) DFT calculations to evaluate the energetic impact of the possible reaction pathways. Figure 4A shows the potential energy profile (enthalpies and Gibbs energies and spin states) for reduction of (dtbbpy)Ni^{II}Br₂ to generate an open coordination site for oxidative addition with the aryl bromide. The energy barrier from the (dtbbpy)Ni^IBr intermediate (C) through TS 1 to give the (dtbbpy)Ni^{III}(Ar)Br₂ intermediate (**D**) is only 6.2 kcal/mol (ΔH^{\ddagger}) and 7.8 kcal/mol (ΔG^{\ddagger}). The 3D depictions of this oxidative addition process is displayed in Figure 5. From **D**, there are several different avenues to generate the homo-coupling biaryl product. We first examined ligand exchange between two **D** (Figure 4B). It requires a Gibbs energy change of 14.8 kcal/mol to form (dtbbpy)Ni^{III}(Ar)₂Br (F) and (dtbbpy)Ni^{III}Br₃ (G). After this ligand exchange step, the reductive elimination requires only 3.9 kcal/mol energy barrier through TS 2. While this is a reasonable energy barrier for the room temperature reaction, our experimental studies indicate that **D** is rapidly converted to Ni^{II}(Ar) intermediate (E) (Scheme 2). Therefore, this Ni^{III}(Ar)-based homo-coupling pathway is less possible. Our calculations are also consistent the possibility that **D** is converted to a E. Figure 4A shows that reduction and bromide loss of D result in E is exothermic and exergonic by 12.1 kcal/mol.

Because of the fast Ni^{III}(Ar) (**D**) to Ni^{II}(Ar) (**E**) conversion, we then examined several biaryl forming pathways from **E**. Figure 4C shows a possible disproportionation route between two **E** to form **F** ready for reductive elimination to produce the biaryl product and a low-valent Ni^I species **H**. The energy barrier for this disproportionation is 18.0 kcal/mol, which makes this pathway less favorable. Figure 4D shows a Ni^I(Ar)-based homo-coupling pathway. Under an electrolytic condition, **E** can be electrochemically reduced to Ni^I(Ar) species (**I**) at a cathode. The high-valent **F** is formed via oxidative addition between **I** and aryl halide. Energy barrier for the oxidative

addition reaction is 8.3 kcal/mol. Finally, we identified a lower energy pathway that is shown in Figure 4E. In this pathway, ligand exchange is much more thermodynamically feasible between **E** and the transiently generated **D**. The generation of **A** and **F** from **D** and **E** is very close to thermal neutral. Therefore, the subsequent reductive elimination through **TS 2** has an overall barrier of only 1.9 kcal/mol. This biaryl forming pathway is reasonable considering that under the electrolytic conditions the Ni^I species (**B**) is generated slowly and its concentration is much lower than that in the pre-synthesized sample we studied in Figure 2, which makes the comproportionation reaction between **D** and **H** to produce **E** slow. Therefore, coexist of (dtbbpy)Ni^{II}(Ar)Br₂ (**D**) and (dtbbpy)Ni^{II}(Ar)Br (**E**) is possible in the reaction mixture, enabling the reaction pathway shown in Figure 4E.

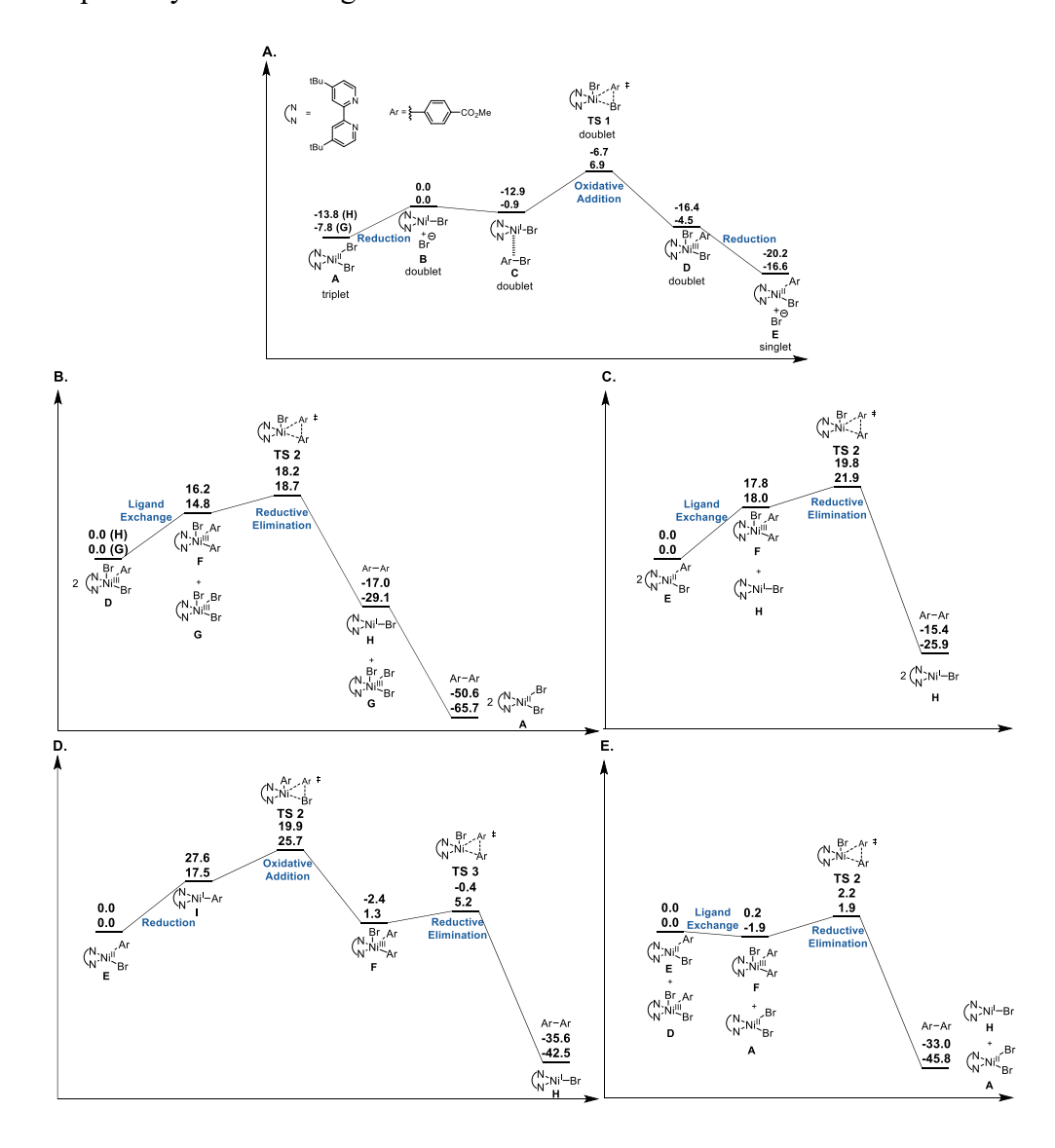


Figure 4. M06-L/6-31G**[LANL2DZ] energy landscapes for the Ni-catalyzed electrochemical aryl bromide homo-coupling.

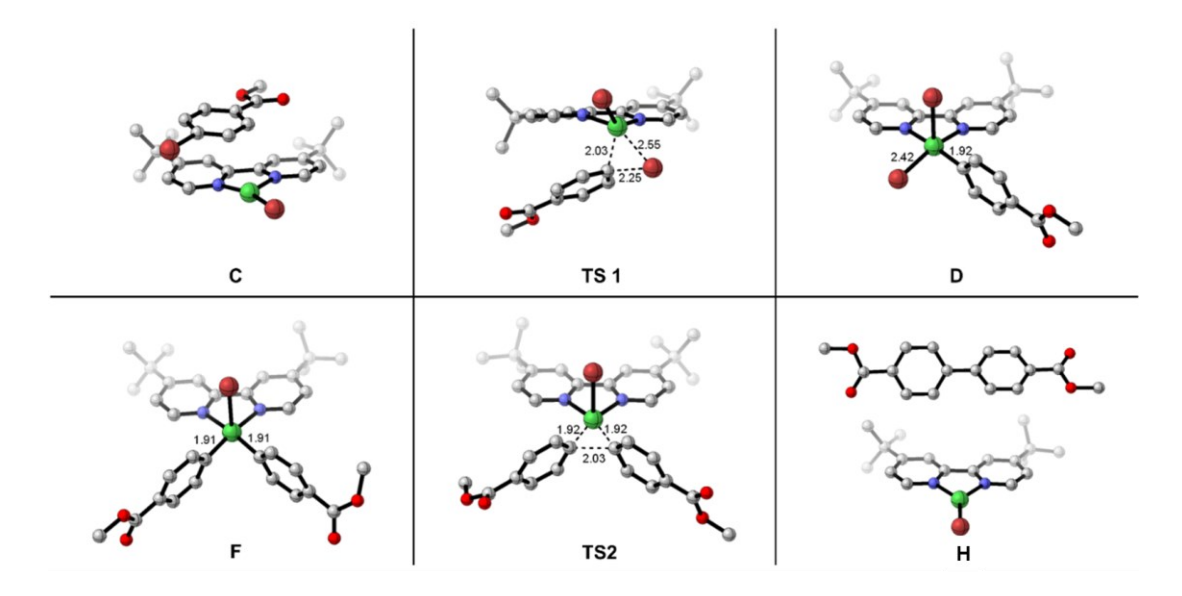


Figure 5. 3D depiction of M06-L structures of the intermediates and transition states for Ni-catalyzed electrochemical aryl bromide homo-coupling.

In summary, we performed experimental and computational studies for mechanistic understandings of Ni-catalyzed electrochemical homo-coupling reaction of aryl halides. The results indicate that an unstable (dtbbpy)Ni^{II}(Ar)Br intermediate formed through oxidative addition of aryl bromide to the cathodically generated Ni^I species and sequent chemical reduction. For electron-rich aryl halides, the oxidative addition reaction rate and homo-coupling reaction efficiency can be enhanced by negatively shifting the redox potential of the Ni-catalyst. DFT computational studies suggest a Ni^{III}(Ar)/Ni^{II}(Ar) bimolecular ligand-exchange pathway for the formation of a high-valence Ni^{III}(Ar)₂ intermediate for reductive elimination and production of the biaryl product. This work reveals the reaction mechanism of Ni-catalyzed electrochemical homo-coupling of aryl halides, which may be of great significance for developing cross-coupling reactions with high selectivity.

Supporting Information contains additional experimental details and figures and tables. Supporting Information is available online or from the author.

Acknowledgements We thank the National Institutes of Health (grant no. R15GM143721) and National Science Foundation (grant no. 1847674) for supporting this study. We acknowledge that the NMR studies are supported by NSF's MRI program (award number 1429195). Arianna Carter was supported through the National Science Foundation Chemistry and Biochemistry REU Site to Prepare Students for Graduate School and an Industrial Career (CHE-2050872).

- (1) Okamoto, K.; Zhang, J.; Housekeeper, J. B.; Marder, S. R.; Luscombe, C. K. C–H Arylation Reaction: Atom Efficient and Greener Syntheses of π -Conjugated Small Molecules and Macromolecules for Organic Electronic Materials. *Macromolecules* **2013**, *46*, 8059-8078.
- (2) Liu, C.; Zhang, H.; Shi, W.; Lei, A. Bond Formations between Two Nucleophiles: Transition Metal Catalyzed Oxidative Cross-Coupling Reactions. *Chemical Reviews* **2011**, *111*, 1780-1824.
- (3) Alberico, D.; Scott, M. E.; Lautens, M. Aryl–Aryl Bond Formation by Transition-Metal-Catalyzed Direct Arylation. *Chemical Reviews* **2007**, *107*, 174-238.
- (4) Pouliot, J.-R.; Grenier, F.; Blaskovits, J. T.; Beaupré, S.; Leclerc, M. Direct (Hetero)arylation Polymerization: Simplicity for Conjugated Polymer Synthesis. *Chemical Reviews* **2016**, *116*, 14225-14274.
- (5) Waldvogel, S. R.; Lips, S.; Selt, M.; Riehl, B.; Kampf, C. J. Electrochemical Arylation Reaction. *Chemical Reviews* **2018**, *118*, 6706-6765.
- (6) Yan, M.; Kawamata, Y.; Baran, P. S. Synthetic Organic Electrochemical Methods Since 2000: On the Verge of a Renaissance. *Chemical Reviews* **2017**, *117*, 13230-13319.
- (7) Luo, J.; Hu, B.; Wu, W.; Hu, M.; Liu, T. L. Nickel-Catalyzed Electrochemical C(sp3)–C(sp2) Cross-Coupling Reactions of Benzyl Trifluoroborate and Organic Halides**. *Angewandte Chemie International Edition* **2021**, *60*, 6107-6116.
- (8) Li, C.; Kawamata, Y.; Nakamura, H.; Vantourout, J. C.; Liu, Z.; Hou, Q.; Bao, D.; Starr, J. T.; Chen, J.; Yan, M.; Baran, P. S. Electrochemically Enabled, Nickel-Catalyzed Amination. *Angewandte Chemie International Edition* **2017**, *56*, 13088-13093.
- (9) Perkins, R. J.; Pedro, D. J.; Hansen, E. C. Electrochemical Nickel Catalysis for Sp2-Sp3 Cross-Electrophile Coupling Reactions of Unactivated Alkyl Halides. *Organic Letters* **2017**, *19*, 3755-3758.
- (10) Jiao, K.-J.; Liu, D.; Ma, H.-X.; Qiu, H.; Fang, P.; Mei, T.-S. Nickel-Catalyzed Electrochemical Reductive Relay Cross-Coupling of Alkyl Halides to Aryl Halides. *Angewandte Chemie International Edition* **2020**, *59*, 6520-6524.
- (11) Peng, L.; Li, Y.; Li, Y.; Wang, W.; Pang, H.; Yin, G. Ligand-Controlled Nickel-Catalyzed Reductive Relay Cross-Coupling of Alkyl Bromides and Aryl Bromides. *ACS Catalysis* **2018**, *8*, 310-313.
- (12) Hamby, T. B.; LaLama, M. J.; Sevov, C. S. Controlling Ni redox states by dynamic ligand exchange for electroreductive Csp3–Csp2 coupling. *Science* **2022**, *376*, 410-416.

- (13) Truesdell, B. L.; Hamby, T. B.; Sevov, C. S. General C(sp2)–C(sp3) Cross-Electrophile Coupling Reactions Enabled by Overcharge Protection of Homogeneous Electrocatalysts. *Journal of the American Chemical Society* **2020**, *142*, 5884-5893.
- (14) Mo, Y.; Lu, Z.; Rughoobur, G.; Patil, P.; Gershenfeld, N.; Akinwande, A. I.; Buchwald, S. L.; Jensen, K. F. Microfluidic electrochemistry for single-electron transfer redoxneutral reactions. *Science* **2020**, *368*, 1352-1357.
- (15) Li, H.; Breen, C. P.; Seo, H.; Jamison, T. F.; Fang, Y.-Q.; Bio, M. M. Ni-Catalyzed Electrochemical Decarboxylative C–C Couplings in Batch and Continuous Flow. *Organic Letters* **2018**, *20*, 1338-1341.
- (16) Koyanagi, T.; Herath, A.; Chong, A.; Ratnikov, M.; Valiere, A.; Chang, J.; Molteni, V.; Loren, J. One-Pot Electrochemical Nickel-Catalyzed Decarboxylative Sp2–Sp3 Cross-Coupling. *Organic Letters* **2019**, *21*, 816-820.
- (17) Kawamata, Y.; Vantourout, J. C.; Hickey, D. P.; Bai, P.; Chen, L.; Hou, Q.; Qiao, W.; Barman, K.; Edwards, M. A.; Garrido-Castro, A. F.; deGruyter, J. N.; Nakamura, H.; Knouse, K.; Qin, C.; Clay, K. J.; Bao, D.; Li, C.; Starr, J. T.; Garcia-Irizarry, C.; Sach, N.; White, H. S.; Neurock, M.; Minteer, S. D.; Baran, P. S. Electrochemically Driven, Ni-Catalyzed Aryl Amination: Scope, Mechanism, and Applications. *Journal of the American Chemical Society* **2019**, *141*, 6392-6402.
- (18) Zhu, C.; Kale, A. P.; Yue, H.; Rueping, M. Redox-Neutral Cross-Coupling Amination with Weak N-Nucleophiles: Arylation of Anilines, Sulfonamides, Sulfoximines, Carbamates, and Imines via Nickelaelectrocatalysis. *JACS Au* **2021**, *1*, 1057-1065.
- (19) Zhang, H.-J.; Chen, L.; Oderinde, M. S.; Edwards, J. T.; Kawamata, Y.; Baran, P. S. Chemoselective, Scalable Nickel-Electrocatalytic O-Arylation of Alcohols. *Angewandte Chemie International Edition* **2021**, *60*, 20700-20705.
- (20) Liu, D.; Ma, H.-X.; Fang, P.; Mei, T.-S. Nickel-Catalyzed Thiolation of Aryl Halides and Heteroaryl Halides through Electrochemistry. *Angewandte Chemie International Edition* **2019**, *58*, 5033-5037.
- (21) Wang, Y.; Deng, L.; Wang, X.; Wu, Z.; Wang, Y.; Pan, Y. Electrochemically Promoted Nickel-Catalyzed Carbon–Sulfur Bond Formation. *ACS Catalysis* **2019**, *9*, 1630-1634.
- (22) Condon, S.; Dupré, D.; Falgayrac, G.; Nédélec, J.-Y. Nickel-Catalyzed Electrochemical Arylation of Activated Olefins. *European Journal of Organic Chemistry* **2002**, 2002, 105-111.
- (23) Condon-Gueugnot, S.; Leonel, E.; Nedelec, J.-Y.; Perichon, J. Electrochemical Arylation of Activated Olefins using a Nickel Salt as Catalyst. *The Journal of Organic Chemistry* **1995**, *60*, 7684-7686.
- (24) Walker, B. R.; Sevov, C. S. An Electrochemically-Promoted, Nickel-Catalyzed, Mizoroki-Heck Reaction. *ACS Catalysis* **2019**.
- (25) Sun, G.-Q.; Zhang, W.; Liao, L.-L.; Li, L.; Nie, Z.-H.; Wu, J.-G.; Zhang, Z.; Yu, D.-G. Nickel-catalyzed electrochemical carboxylation of unactivated aryl and alkyl halides with CO2. *Nature Communications* **2021**, *12*, 7086.
- (26) Sun, G.-Q.; Yu, P.; Zhang, W.; Zhang, W.; Wang, Y.; Liao, L.-L.; Zhang, Z.; Li, L.; Lu, Z.; Yu, D.-G.; Lin, S. Electrochemical reactor dictates site selectivity in N-heteroarene carboxylations. *Nature* **2023**, *615*, 67-72.
- (27) Beutner, G. L.; Simmons, E. M.; Ayers, S.; Bemis, C. Y.; Goldfogel, M. J.; Joe, C. L.; Marshall, J.; Wisniewski, S. R. A Process Chemistry Benchmark for sp2–sp3 Cross Couplings. *The Journal of Organic Chemistry* **2021**, *86*, 10380-10396.

- (28) Qiu, H.; Shuai, B.; Wang, Y.-Z.; Liu, D.; Chen, Y.-G.; Gao, P.-S.; Ma, H.-X.; Chen, S.; Mei, T.-S. Enantioselective Ni-Catalyzed Electrochemical Synthesis of Biaryl Atropisomers. *Journal of the American Chemical Society* **2020**, *142*, 9872-9878.
- (29) de França, K. W. R.; Navarro, M.; Léonel, É.; Durandetti, M.; Nédélec, J.-Y. Electrochemical Homocoupling of 2-Bromomethylpyridines Catalyzed by Nickel Complexes. *The Journal of Organic Chemistry* **2002**, *67*, 1838-1842.
- (30) Chen, W.-W.; Zhao, Q.; Xu, M.-H.; Lin, G.-Q. Nickel-Catalyzed Asymmetric Ullmann Coupling for the Synthesis of Axially Chiral Tetra-ortho-Substituted Biaryl Dials. *Organic Letters* **2010**, *12*, 1072-1075.
- (31) Oliveira, J. L.; Silva, M. J.; Florêncio, T.; Urgin, K.; Sengmany, S.; Léonel, E.; Nédélec, J.-Y.; Navarro, M. Electrochemical coupling of mono and dihalopyridines catalyzed by nickel complex in undivided cell. *Tetrahedron* **2012**, *68*, 2383-2390.
- (32) Till, N. A.; Oh, S.; MacMillan, D. W. C.; Bird, M. J. The Application of Pulse Radiolysis to the Study of Ni(I) Intermediates in Ni-Catalyzed Cross-Coupling Reactions. *Journal of the American Chemical Society* **2021**, *143*, 9332-9337.